Cellulose (2015) 22:2245–2261
DOI 10.1007/s10570-015-0648-5

ORIGINAL PAPER

Effects of periodate oxidation on cellulose polymorphs

Martin Siller · Hassan Amer · Markus Bacher · Walter Roggenstein · Thomas Rosenau · Antje Potthast

Received: 5 January 2015 / Accepted: 3 May 2015 / Published online: 15 May 2015

Abstract Since periodate oxidation selectively creates (masked) aldehyde groups that can serve as anchors for further modification steps, this method is suitable for modifying and functionalizing cellulose. Although numerous studies deal with that topic, there are still knowledge gaps regarding periodate oxidation. In our study, we focused on examining how the type of cellulose allomorph influences the reaction. We compared the oxidation of two allomorphs, namely cellulose I, cellulose II and mixtures of cellulose I and II, and examined changes in crystallinity and thermal decomposition behavior. Generally, periodate oxidation proceeded faster in the case of cellulose II samples, followed by the mixed cellulose I/II samples; cellulose I was the slowest. Based on our results, the major influencing factor is the overall crystallinity of the sample. The influence of the allomorph was minor. Crystallinity decreased upon oxidation, but no significant differences were found between the different cellulose polymorphs. Following the crystallinity during the oxidation reaction proved to be very difficult. Determining crystallinity with solid-state nuclear magnetic resonance (NMR) was largely hampered by superposition with new resonances that interfere with crystallinity determination. Structural changes during oxidation as evident from solid-state NMR are discussed in detail. Alternative methods for crystallinity analysis, such as near infrared spectroscopy, attenuated total reflection infrared spectroscopy, and Raman spectroscopy, had similar problems but to a lesser extent, with Raman being the method of choice. Thermogravimetric analysis showed thermal decomposition of oxidized cellulose I and II to be similar. An anomaly was found in the case of oxidized viscose fibers. Slightly oxidized samples showed increased mass loss in the temperature range up to 360 °C whereas higher oxidized samples and all pulp samples showed decreased mass loss.

Keywords Periodate oxidation · Cellulose I · Cellulose II · Crystallinity · Thermogravimetry · Solid-state NMR (CPMAS)

Electronic supplementary material The online version of this article (doi:10.1007/s10570-015-0648-5) contains supplementary material, which is available to authorized users.

M. Siller
Kompetenzzentrum Holz GmbH, Altenberger Straße 69, 4040 Linz, Austria

M. Siller · H. Amer · M. Bacher · T. Rosenau · A. Potthast (✉)
Department of Chemistry, University of Natural Resources and Life Sciences, UFT Campus Tulln, Konrad-Lorenz-Straße 24, 3430 Tulln, Austria
e-mail: antje.potthast@boku.ac.at

H. Amer
Department of Natural and Microbial Products Chemistry, National Research Centre, P.O. 12622, Dokki, Giza, Egypt

W. Roggenstein
Kelheim Fibres GmbH, Regensburger Str. 109, 93309 Kelheim, Germany

Introduction

Functionalized cellulosic products have a high utilization potential in a biobased economy. One method for modifying cellulose is the creation of chemical anchor points—e.g. oxidized groups—for the subsequent attachment of functional molecules. An overview about various oxidation methods, suitable for that purpose, can be found in a review by Coseri et al. (2013). Aldehyde groups, are versatile functional groups as they can serve not only as hooks to attach amine molecules as imines (Schiff bases) but can be used for a number of subsequent reactions including oxidation to carboxyl groups. A widely studied method for generating aldehyde groups in cellulose is the periodate oxidation approach. Periodate (IO_4^-) forms an iododioxolan intermediate with vicinal bisequatorial hydroxyl groups and breaks the C–C bond between the corresponding carbons, such as that between C-2 and C-3 in cellulose, thus formally creating two aldehyde groups. Therefore, periodate oxidation of cellulose is a selective modification that cleaves the cellulose's glucopyranoside rings between C-2 and C-3 yielding 2,3-dialdehyde cellulose (DAC; Malaprade 1928; Jackson and Hudson 1938). The aldehyde functionalities produced by periodate oxidation are not present in their free form but in a complex, interconverting mixture of hydrates, as well as intramolecular and intermolecular hemiacetals (hemialdals). Therefore, the aldehyde CHO groups of DAC are largely invisible on infrared (IR) and nuclear magnetic resonance (NMR) spectra (Fan et al. 2001; Vicini et al. 2004).

The oxidation rate is strongly influenced by periodate concentration, temperature and the presence of metal salts (Varma and Kulkarni 2002; Sirvio et al. 2011). The reaction on cellulose is usually performed with sodium metaperiodate under mildly acidic conditions (pH 2–5) (Jayme and Maris 1944; Varma and Kulkarni 2002). Although periodate oxidation is a specific reaction, some undesired side reactions, such as overoxidation (Hudson and Barker 1967), photodecomposition of periodate (Symons 1955) or iodine formation (Sirvio et al. 2011), may occur. Additionally, DAC degrades fast under alkaline conditions due to the β-alkoxy elimination reactions (Whistler et al. 1959). This reaction can also be used as a diagnostic tool for evaluating oxidation degrees and patterns (Stefanovic et al. 2013; Ahn et al. 2013).

Periodate oxidation has been studied for several decades, but questions remain. The kinetic stages of periodate oxidation reactions, the time when crystalline regions are attacked compared to the amorphous counterparts and the influence of cellulose polymorphism are still debated. The situation is complicated by the numerous analytical techniques and data evaluation methods applied to the issue. For instance, the crystallinity indices (CIs) found in the literature show high variations depending on the method and calibration used (Nelson and O'Connor 1964; Park et al. 2010). The most common method for determining the crystallinity of cellulose is wide-angle X-ray scattering (WAXS, also wide-angle X-ray diffraction, WAXD); many variations of the original method are used regularly today (Hermans and Weidinger 1948; Segal et al. 1959; Vonk 1973; Fink et al. 1985; Garvey et al. 2005). Other techniques for determining CIs include mid-infrared spectroscopy (IR; Nelson and O'Connor 1964; Baldinger et al. 2000), near-infrared spectroscopy (Basch et al. 1974), Raman spectroscopy (Schenzel and Fischer 2004; Schenzel et al. 2005), density measurements, accessibility from the moisture regain (Nelson and O'Connor 1964), differential scanning calorimetry (DSC; Ciolacu et al. 2011) and solid-state ^{13}C NMR spectroscopy (Larsson et al. 1997; Newman 2004; Park et al. 2009).

The different structure of the various cellulose allomorphs causes differences in their reactivity in oxidation reactions. Oxidation reactions on cellulose can be quite sensitive to the allomorph used as the starting material; here we consider only the most common forms of cellulose I (native cellulose), cellulose II (regenerated or mercerized cellulose) and their mixtures (cellulose I + II). A vivid example of the influence of cellulose allomorphism on the conversion rate is the oxidation with 2,2,6,6-tetramethylpiperidine-1-oxyl radical (TEMPO); cellulose I is much less reactive than cellulose II. The latter can be quantitatively converted into the corresponding polyglucuronic acid while the former cellulose I can be oxidized only to some extent, leaving a non-oxidized residue behind (Isogai and Kato 1998).

Many studies have shown that periodate oxidation causes a continuous decrease in crystallinity (Rowland and Cousins 1966; Varma et al. 1985; Varma and Chavan 1995a; Kim et al. 2000; Meng et al. 2005; Calvini et al. 2006b). This indicates that periodate can easily oxidize the crystalline regions of cellulose,

yielding amorphous cellulose. In contrast, algal cellulose maintained high crystallinity even at high degrees of oxidation (Kim et al. 1999). Xu and Huang (2011) reported a slight increase in crystallinity after very weak periodate oxidation probably caused by partial dissolution of the oxidized fraction, which would argue in favor of a preferred attack on amorphous material. Dash et al. (2012) did not observe changes in the crystallinity of cellulose nano whiskers after weak periodate oxidation and subsequent reductive amination. Rowland and Cousins (1966) observed a progressive decrease in the CI, following a pseudo zero-order reaction indicating a diffusion-controlled process. Thus, they suggested that the initial attack mainly happened in the amorphous regions or on surfaces. Calvini et al. (2006a, b) concluded from kinetic considerations that crystalline regions are affected as well as amorphous ones from the beginning of the oxidation process by a constant but slower rate. The researchers concluded that the amorphous regions are oxidized during the first phase before the slow second reaction and the even slower third reaction cause oxidation of the surface and the inner core of crystallites, respectively. Similar conclusions were made by Maekawa et al. (1986), Varma and Chavan (1995a), Margutti et al. (2002) and Liu et al. (2012). However, Varma et al. (1985) found a decrease in crystallinity proportional to the degree of oxidation indicating that oxidation proceeded nearly equally in amorphous and crystalline regions. Using carbonyl-selective fluorescence labeling (CCOA method), we showed in previous work that the attack on the crystalline regions started early along the oxidation path, long before the amorphous regions were fully oxidized (Potthast et al. 2007). As this brief literature review shows, the available reports on periodate oxidation and cellulose allomorphs are far from consistent, not to say highly contradictory.

Periodate oxidation also has a large influence on the thermal decomposition properties of cellulose. Thermal degradation of cellulose can be divided into three phases: First, moisture and volatiles are released below 290 °C, followed by the main degradation comprising thermal scissions of glycosidic bonds, formation of carbonyl or carboxyl groups followed by decarbonylation and decarboxylation, and production of levoglucosan, condensation and charring products. In the third phase, carbonization occurs (Tang and Bacon 1964; Shafizadeh 1982; Sefain and El-Kalyoubi 1984; Li et al. 2007). Thermogravimetric analysis (TGA) showed that the decomposition of DAC from cellulose I starts at lower temperatures, but proceeds more slowly, which is why at higher temperatures DAC is more stable than unmodified cellulose (Varma and Chavan 1995a, b; Kim and Kuga 2001; Vicini et al. 2004). The thermal properties of periodate oxidized cellulose II samples have not been studied thus far.

In this study, we systematically examined the influence of cellulose allomorphism on periodate oxidation of cellulose but limited to the technically important I- and II-allomorph. We focused on crystallinity effects and thermal stability. Different methods for determining crystallinity have been evaluated for their applicability to periodate-oxidized cellulose samples. The question whether the observed large differences between cellulose I and II on TEMPO oxidation are also effective in the case of periodate oxidation, is examined.

Materials and methods

Cellulose samples

The cellulosic starting materials for the experiments were cellulose I pulp (bleached beech sulfite-dissolving pulp: Lenzing AG, Lenzing, Austria) and cellulose II fiber (viscose (rayon) fibers: bleached, desulfurized, 1.7 dtex, without textile finish, (Kelheim Fibres GmbH, Kelheim, Germany). Cellulose I pulp has a brightness of 92.2 % ISO (TAPPI test method T452 om-98), a kappa number of 0.43 (TAPPI Test method T236 cm-85) and a 93.4 % residue in 18 % NaOH (DIN 54355) (Henniges et al. 2012). Weight average molar mass was ~290 and ~65 kg/mol for cellulose I pulp and cellulose II fiber, respectively; details about the molar mass distribution of the pulp and fiber samples can be found in Henniges et al. (2011) and Siller et al. (2014). Pulp and viscose fiber samples were cut into small pieces and disintegrated in a kitchen blender.

Mercerization

The cellulose I pulp sample was mercerized in sodium hydroxide (NaOH) solutions of different concentrations to achieve a partial or complete conversion to cellulose II. For full conversion to cellulose II, 20 % NaOH solutions were used, and 10 % NaOH solutions for

incomplete conversion (cellulose I/II mix). Mercerization was performed at room temperature with 25 g pulp in 1 l of sodium hydroxide solution of the appropriate concentration. Samples were filtered and washed to neutral with water after 4 h reaction time, and were dried at 50 °C. Effects of alkalization of this pulp sample on molar mass distribution and carbonyl group content have been described earlier (Potthast et al. 2003).

Periodate oxidation

Pulp (cellulose I), mercerized pulp (cellulose I and cellulose I/II mix) and viscose (cellulose II fiber) samples were oxidized with sodium metaperiodate ($NaIO_4$) solutions to a degree of oxidation (DO = percentage of oxidized anhydroglucose units based on target periodate consumption) of 12.5, 25, 50 and 100 %. The progress of the reaction was followed with ultraviolet (UV) spectroscopy to measure the absorption of the supernatant at 290 nm according to Maekawa et al. (1986). Reactions were performed at room temperature in the dark on a shaker. A stoichiometric amount of oxidant with a concentration of 5 mg $NaIO_4$/ml was used for the 12.5, 25 and 50 % DO samples. An excess of oxidant was used for the fully oxidized samples (100 % DO; cf. Table 1 for detailed conditions). Reactions were stopped with filtration and washing on a Büchner funnel when the consumption of periodate levelled off (usually at yields significantly above 95 %). Details of the experimental setup and reaction conditions are described in Fig. 1 and Table 1.

Reduction of dialdehyde cellulose

Oxidized cellulose sample (1.0 g) was added to a cooled solution of 1.0 g sodium borohydride in 50 ml of deionized water. The reaction mixture was stirred overnight at 4 °C and then quenched by addition of 2.0 ml of acetic acid. The product was dialyzed [molecular weight cut-off (MWCO) = 13,000 Da] against deionized water for 48 h and then lyophilized.

Spectroscopic analysis

Ultraviolet spectroscopy (UV)

To quantify periodate, UV spectra were measured with a Perkin Elmer Lambda 35 UV/Vis Spectrometer at 290 nm. Linear calibration was obtained with standard solutions of sodium metaperiodate in the range from 0.1 to 5 mM.

Near-infrared spectroscopy (NIR)

Measurements were performed with a Bruker MPA Multi-Purpose Analyzer with a fiber optic probe and a Te-InGaAs detector (10 kHz). Cellulose samples were conditioned in the measuring room for one week. Each sample was measured in triplicate with 32 scans 12,500–4000 cm^{-1} with a resolution of 8 cm^{-1}. OPUS 7.0 software was used to evaluate the data, and the spectra were baseline corrected (Rubberband correction) and exported. Further data processing was done with Origin software: The average spectra were calculated from the triple measurements, spectra were normalized at 5187 cm^{-1} and the peak height and area were calculated for the peaks at 5187 and 4760 cm^{-1}. The CI was calculated as described by Basch et al. (1974) from the peak heights (H):

$$CI(NIR) = H_{4760}/(H_{4760} + H_{5190}).$$

A similar trend was observed if peak areas were used to calculate the CI.

Attenuated total reflection infrared spectroscopy (ATR-IR)

IR spectra were recorded with a Perkin Elmer FT-IR Spectrometer Frontier equipped with a Universal ATR Sampling Accessory. Each sample was scanned in quadruplicate from 4000 to 650 cm^{-1} with a resolution of 4 cm^{-1}. Spectra were baseline corrected and exported. Peak height and peak area were calculated with Origin 8.1 for the peaks at 1370 and 2900 cm^{-1}. The CI was calculated from the ratio of the peak heights (H) of the two peaks (Nelson and O'Connor 1964):

$$CI(ATR) = H_{1370}/H_{2900}.$$

Raman spectroscopy

Each sample was measured four times with a Bruker MultiRam spectrometer (NdYag Laser 1064 nm, 500 mW). Data were evaluated with OPUS 7.0 Software in the range 2.4–4000 cm^{-1}. Spectra were averaged and baseline corrected. The cellulose I content and

Table 1 List of samples used in this study and respective crystallinity index

Polymorph	Degree of oxidation (%)	Periodate oxidation	Cellulose I content by Raman (%)	Crystallinity index					
				NMR simple integration	NMR peak fitting	NIR	ATR-IR	Raman cellulose I method	Raman cellulose II method
Cellulose I	–	–	95	0.54	0.53	0.51	0.73	0.54	
	12.5	5 mg $NaIO_4$/ml, 3 % cellulose	87			0.47	0.59	0.52	
	25	5 mg $NaIO_4$/ml, 1.5 % cellulose	84			0.43	0.61	0.51	
	50	5 mg $NaIO_4$/ml, 0.75 % cellulose	80			0.36	0.42	0.47	
	100	1.14 equivalent, 21 mg $NaIO_4$/ml, 1.4 % cellulose	91			0.28	0.19	0.44	
Cellulose I/II mix	–	–	39	0.65	0.61	0.45	0.69	0.47	
	12.5	5 mg $NaIO_4$/ml, 3 % cellulose	43			0.40	0.69	0.46	
	25	5 mg $NaIO_4$/ml, 1.5 % cellulose	49			0.37	0.56	0.46	
	50	5 mg $NaIO_4$/ml, 0.75 % cellulose	63			0.33	0.46	0.45	
	100	1.14 equivalent, 21 mg $NaIO_4$/ml, 1.4 % cellulose	95			0.28	0.19	0.43	
Cellulose II pulp	–	–	5	0.58	0.61	0.42	0.63	0.44	0.43
	12.5	5 mg $NaIO_4$/ml, 3 % cellulose	6			0.39	0.69	0.44	0.38
	25	5 mg $NaIO_4$/ml, 1.5 % cellulose	1			0.35	0.63	0.43	0.34
	50	5 mg $NaIO_4$/ml, 0.75 % cellulose	6			0.32	0.51	0.42	0.17
	100	1.14 equivalent, 21 mg $NaIO_4$/ml, 1.4 % cellulose	49			0.28	0.18	0.43	
Cellulose II fiber	–	–	−2	0.53	0.50	0.39	0.54	0.44	0.35
	12.5	5 mg $NaIO_4$/ml, 3 % cellulose	−3			0.37	0.40	0.43	0.30
	25	5 mg $NaIO_4$/ml, 1.5 % cellulose	−2			0.34	0.45	0.44	0.23
	50	5 mg $NaIO_4$/ml, 0.75 % cellulose	6			0.31	0.39	0.44	0.13
	100	1.25 equivalent, 22 mg $NaIO_4$/ml, 1.3 % cellulose	67			0.24	0.19	0.45	

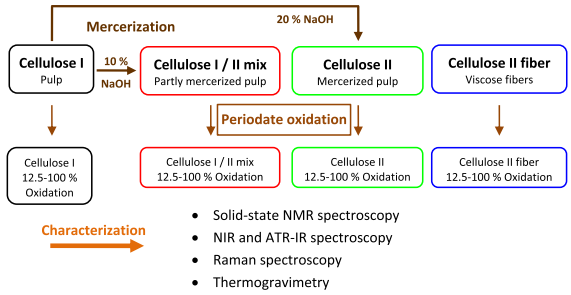

Fig. 1 Experimental setup of mercerization and periodate oxidation of pulp and viscose fibers

crystallinity were calculated with chemometric methods calibrated with WAXS data [internal method Lenzing AG and Röder et al. (2006a, b)]. One chemometric method was used for the cellulose I samples and cellulose I/II mixed samples, and a special method for cellulose II samples was used when the cellulose I content was below 10 %.

Solid-state ^{13}C NMR

All solid-state NMR experiments were performed on a Bruker Avance III HD 400 spectrometer (resonance frequency of ^{1}H of 400.13 MHz, and ^{13}C of 100.61 MHz), equipped with a 4 mm dual broadband cross-polarization magic angle spinning (CPMAS) probe. The samples were swollen overnight in deionized water before measurement. ^{13}C spectra were acquired with the total sideband suppression (TOSS) sequence at ambient temperature with a spinning rate of 5 kHz, a cross-polarization (CP) contact time of 2 ms, a recycle delay of 2 s, SPINAL-64 ^{1}H decoupling and an acquisition time of 43 ms. Chemical shifts were referenced externally against the carbonyl signal of glycine at $\delta = 176.03$ ppm. The acquired free induction decays (FIDs) were apodized with an exponential function (lb = 11 Hz) before the Fourier transformation. Peak fitting was performed with the Dmfit program (Massiot et al. 2002). Cellulose samples were fitted in the C6 region (59–68 ppm) since this gave better fitting results for cellulose II samples. In addition to peak fitting, CIs were calculated using simple integration. Integration was done at C6 (approximately 64–69 ppm = crystalline cellulose I, approximately 62–65 ppm = crystalline cellulose II, approximately 58–62 = amorphous cellulose). The crystallinity index was then calculated from the ratio between the area of the cellulose I and cellulose II peak to the total area of the peak.

Liquid NMR

Liquid NMR spectra were recorded on a Bruker Avance II 400 (resonance frequencies 400.13 MHz for ^{1}H and 100.61 MHz for ^{13}C) equipped with a 5 mm observe broadband probe head (BBFO) with z-gradients at room temperature with standard Bruker pulse programs. The samples were dissolved in 0.6 ml of D_2O (99.8 % D, eurisotop). For referencing the spectra, 4,4-dimethyl-4-silapentane-1-sulfonic acid (DSS) was added as internal standard. ^{1}H NMR data were collected with 32 k complex data points and apodized with a Gaussian window function (lb = −0.3 Hz and gb = 0.3 Hz) prior to Fourier transformation.

Thermogravimetry

Thermogravimetric measurements were performed with a Netzsch TG209 F1 instrument under air at a heating rate of 20 K/min.

Cellulose II fiber samples were cut into small pieces before the measurements to reduce noise. Each sample was measured in duplicate, and the curves were averaged. The first derivative was calculated to facilitate data interpretation; a smoothing procedure was applied for this calculation.

The weight loss data were calculated relative to residual mass at 150 °C to eliminate the influence of different moisture content.

Results and discussion

To determine whether different polymorphs respond differently to periodate oxidation, the reaction kinetic of cellulose I oxidation (bleached beech sulfite pulp) and cellulose II oxidation (either viscose fibers produced from that pulp via xanthation, dissolution and regeneration or cellulose II from that pulp by mercerization) with sodium metaperiodate was recorded, based on monitoring the periodate consumption. In addition to the pure allomorphs, cellulose I/II mixtures obtained with partial mercerization were used (cf. Fig. S1 in the supplement for the CPMAS spectra of the starting materials). All samples were

oxidized to different degrees, 12.5, 25, 50 and 100 %, calculated again based on periodate consumption. Figure 1 gives an overview of the different materials investigated. The oxidation procedure was quite well reproducible (standard deviation of 0.32 (N = 3; relative standard deviation = 1.4 %) for 23.7 % DO after 50 h, cellulose I sample) provided that the temperature was kept constant (cf. Fig. 2). Periodate oxidation causes a slight mass loss—e.g. a mass yield of ~90 % was found for cotton linters with 50 % DO; similar can be expected for pulp and fiber samples.

Comparison of the reaction rates for the different cellulose allomorphs gave a clear result: The cellulose I sample was oxidized more slowly than its partly or fully mercerized counterparts (cellulose I/II mix; cellulose II pulp; cellulose II fiber). From the very beginning of the oxidation process, the cellulose II fiber sample reacted at the highest rate. In general, we observed a clear graduation from cellulose II being the fastest to be oxidized to pure cellulose I being the slowest. Just mercerized cellulose II pulp reacted more slowly than the cellulose II fiber.

A linear relation between the natural logarithm of the periodate concentration and the reaction time was observed for the first 7–8 days of oxidation (cf. inset graph in Fig. 2). This shows that the oxidation follows a pseudo first order reaction with respect to periodate concentration.

An additional experiment was done to verify the degree of oxidation that was estimated from the photometrically determined periodate consumption. A highly oxidized cellulose I pulp sample (DO = 93.7 % according to periodate consumption) was reduced with sodium borohydride. This reductive treatment creates primary alcohol groups at the C-2 and C-3 position and removes aldehydes, aldehyde hydrates, hemialdals and hemiacetals. This simplifies the structure of the molecule and gives a water soluble product that can be analyzed by liquid NMR (cf. Fig. 3). Oxidized and reduced units can be distinguished from non-oxidized anhydroglucose units by the signal from the proton at C-1. In case of a non-oxidized unit this proton gives a doublet at 4.59 ppm whereas a triplet at 4.92 ppm is obtained in case of an oxidized and subsequently reduced unit. Integration of these peaks gave an area ratio of 0.93:0.07 between the respective triplet and doublet. Thus the degree of oxidation determined by NMR (93 %) fits very well the DO estimated from periodate consumption (93.7 %). Hence, we can conclude that the calculation

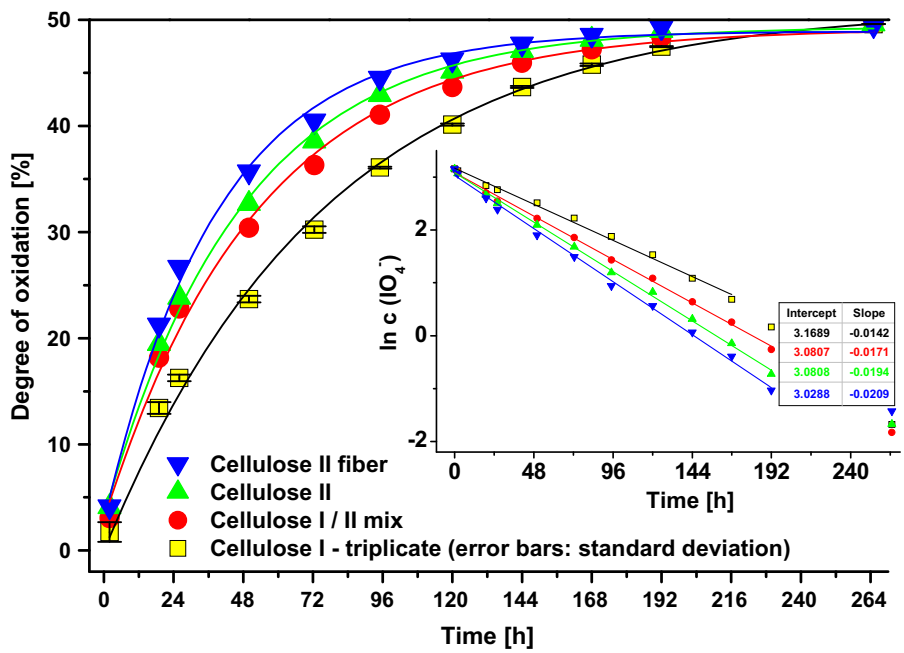

Fig. 2 Time course of periodate oxidation for 50 % degree of ring opening; *inset graph* shows the first order reaction kinetics with respect to periodate concentration

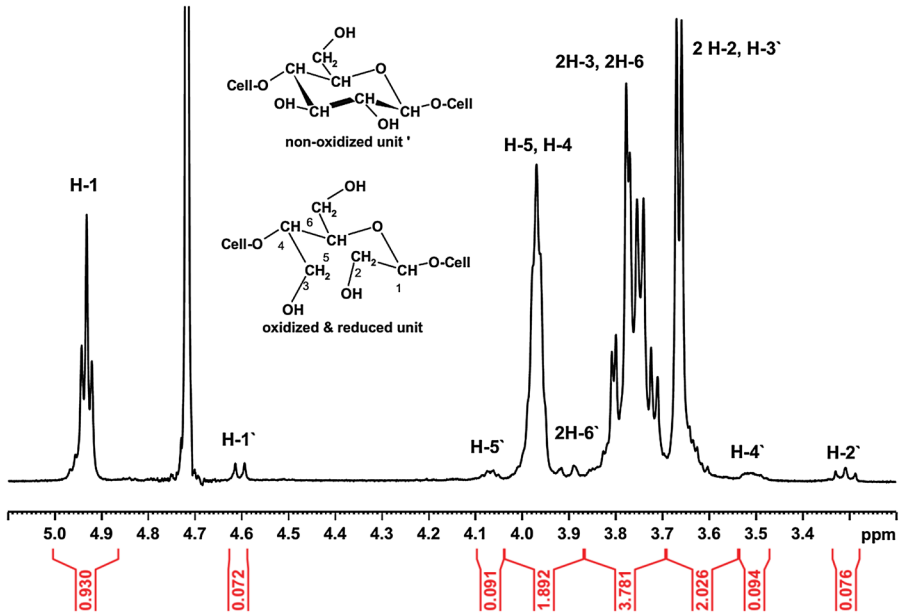

Fig. 3 ^{1}H-NMR spectrum of a periodate oxidized and subsequently reduced cellulose I sample used for quantification of the degree of oxidation. Assignment depicted as prime (′) refer to the non-oxidized anhydroglucose unit

Table 2 Amounts of crystalline and amorphous cellulose in the samples, as determined by solid-state NMR (based on peak fitting on carbon C6) and Raman spectroscopy (in parenthesis)

Sample	Treatment	Crystalline		Amorphous (%)
		Cellulose I (%)	Cellulose II (%)	
Cellulose I pulp	–	53	–	47 (46)
Cellulose I/II mix	10 % NaOH	15	46	39 (53)
Cellulose II	20 % NaOH	4	57	39 (57)
Cellulose II fiber	Regeneration	–	50	50 (65)

of the DO from the periodate consumption gives sufficiently accurate data.

The observed higher reactivity of cellulose II raised the question whether the polymorphism, that is, the differences in the crystal structure, is the driving force behind these clear differences in reaction rates or simply the degree of crystallinity—independent of the crystal form. The pulp used in the study is a dissolving pulp that shows high reactivity in viscose production and direct dissolution in several cellulose solvents; that is, it should be well accessible to chemical reagents and undergo derivatization quickly in general. As discussed in the introduction, a faster reaction rate for cellulose II was also described by Maekawa et al. (1986) and was attributed to the lower overall crystallinity of those samples, assuming the crystalline regions were oxidized more slowly than the amorphous ones. To eliminate crystallinity as the influencing factor, we first analyzed the samples with CPMAS. According to this measurement (cf. Table 2), cellulose I and the viscose sample used in this study have an CI around 50 % (53 vs. 50 %). The CI describes the proportion of crystalline cellulose within the total sample. However, the cellulose samples clearly behaved differently, and the regenerated cellulose II sample reacted the fastest. Possible reasons for that overall better accessibility of cellulose II might be that cellulose II crystals are better accessible to the periodate anion compared to the cellulose I counterparts or a higher accessibility of the amorphous regions. From the faster reaction of cellulose II, we must conclude that the type of allomorph plays a more decisive role than the degree of crystallinity.

Now the mixed crystal forms become of interest, which were produced by partial mercerization of the cellulose I sample. Mercerization caused a slight increase in overall crystallinity. The CI for the partly mercerized sample cellulose I/II and the completely mercerized sample were about 10 % higher than that of the starting material based on the NMR CI determination. This does not agree with the literature data in which mercerization was described as accompanied by a decrease in crystallinity (Hermans and Weidinger 1948; Ranby 1952; Ant-Wuorinen 1955). Thus, we have analyzed the crystallinity with other means, in order to consolidate the NMR data. Although the fitting procedure worked well for cellulose I, obtaining reliable data for mixed crystals and cellulose II is more difficult (cf. Table 2). The situation changed when the degree of crystallinity was analyzed with Raman spectroscopy (based on calibration with WAXS, cf. Tables 1, 2). Cellulose I showed the highest crystallinity followed by the cellulose I/II mix and the cellulose II fiber with the lowest CI. Based on these results, the degree of crystallinity is the driving force behind the observed reaction rate (cf. Fig. 2). The differences in the oxidation speed followed the crystallinity trend determined with Raman spectroscopy.

Overall, the fast conversion of the viscose fiber was a surprise. In viscose fibers, high orientation is induced by the spinning process, which usually slows down the chemical reactions or dissolution processes of these materials to a large extent (Siller et al. 2014). Accessibility is also reduced due to the core–sheath structure. However, the rate order observation is in line with that for lower Raman crystallinity and the TEMPO case, which also showed higher reactivity for cellulose II. However, in contrast to TEMPO, periodate oxidation finally reached 100 % of the expected value in all cases independent of polymorphism or morphology, whereas in the TEMPO oxidation process of cellulose I there was a point of decreased reactivity from which oxidation levels off. It has been shown for TEMPO oxidation that oxidized residues were introduced only in amorphous regions and on crystallite surfaces without affecting crystallinity or crystallite size (Saito and Isogai 2004). The higher reactivity of cellulose II has been explained by higher accessibility due to lower crystallinity and differences in hydrogen bonding patterns at the C6 hydroxyl group (Isogai and Kato 1998). For periodate, the oxidation process runs all the way through to full oxidation and thus affects the crystalline regions throughout.

When different polymorphs with different degrees of crystallinity were considered, the way crystallinity is determined plays a role. Thus, we also tested different approaches for analyzing the degree of crystallinity in periodate-oxidized samples. In general, the oxidation process brings very pronounced changes to the cellulose structure due to the oxidative glucopyranose ring opening and subsequent intermolecular and intramolecular hemiacetal formation with concomitant ample crosslinking possibilities.

In CPMAS, oxidation caused additional resonances and shifts of peaks as expected, as was described by Varma et al. (1997). The spectra from samples up to the 50 % degree of the ring opening retained some similarity to those of the starting materials, whereas the spectra of fully oxidized samples changed profoundly as expected (cf. Fig. 4 and Fig. S2 in the supplement). Interestingly, fully oxidized samples of different origin did not give identical spectra but retained some characteristics of the respective starting material (cf. Fig. S3 in the supplement).

Changes in crystallinity, if they occurred, could not be reliably reported with CPMAS since the peaks were superimposed by overlapping effects. Proietti et al. (2004) attributed additional signals in the range from 90 to 100 ppm to cellulose oligomers. This appears less likely since the anomeric carbons of these oligomers do not resonate very differently from those in cellulose. Instead, the C2 and C3 "aldehyde" groups of dialdehyde cellulose are present as hydrates, hemiacetals or hemialdals that also appear in this shift area. This also explains the absence of a "typical" carbonyl/aldehyde resonance between 175 and 185 ppm (Kim et al. 2000). The aldehyde functionalities are nearly completely present in those masked forms, but not as genuine aldehydes with sp^2 carbons (i.e., with double-bonded oxygen).

Different methods have been described in the literature for calculating CIs from ^{13}C solid-state NMR spectra. The signals from C4 of the glucopyranose rings are often used to determine CIs since the resonances from the crystalline and amorphous regions are well resolved (Newman 2004). Another option is the peak deconvolution method with Gaussian and Lorentzian curves from individual contributors fitted in such a way that they accumulate to the overall spectrum. These overlapping curves have

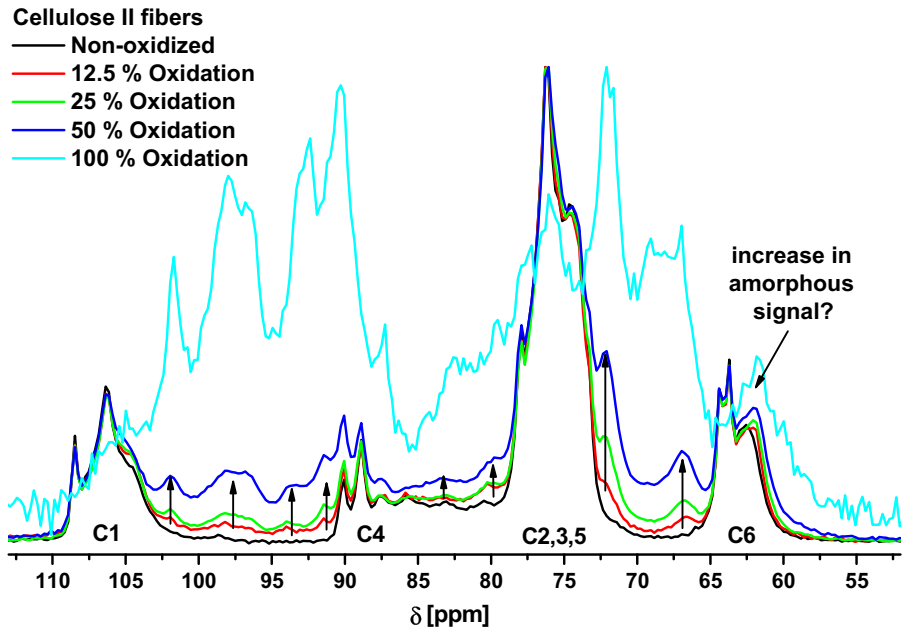

Fig. 4 Solid-state NMR spectra of a periodate oxidation series with cellulose II fibers

been assigned to different sources: Iα, para-crystalline, I(α + β), Iβ, accessible fibril surfaces and inaccessible fibril surfaces. The degrees of crystallinity are then calculated from the ratio of these cellulose fractions according to published protocols (Larsson et al. 1997, 1999; Wickholm et al. 1998; Zuckerstätter et al. 2009).

Peak fitting for periodate-treated celluloses cannot be based on the C4 resonance region, which is directly and strongly influenced by the changes in the chemical environment brought about by this oxidation. Due to the many different chemical structures produced by intra- and intermolecular crosslinking and hydratization, assignment and deconvolution would be impossible.

Using the C6 region would the logical choice since this carbon atom is not directly affected and has the largest distance to the oxidatively changed reaction centers C-2 and C-3. Often, simple integration of the C6 resonance in the range between 59 and 68 ppm is used: The peak area between 65 and 68 ppm is attributed to crystalline cellulose I, the peak between 63 and 65 to crystalline cellulose II, and the region more upfield to amorphous cellulose. The crystallinity index is then calculated from the ratio between the area sum of cellulose I and cellulose II in relation to the total C6 integral. Unfortunately, this approach is not possible for periodate-oxidized material. Internal crosslinking involving C-6 hydroxyls, which is visible in the spectra in Fig. 4, also disrupts this approach. The newly appearing resonances in the range of about 65–69 ppm, which increase as the degree of oxidation increases, originate from C6 involved in hemiacetal structures. The C6-OH moiety is thus increasingly engaged in forming that C6–O–CH(R)–O structures that account for the observed downfield shift. That these resonances at about 65–68 ppm agree with the shifts in the cellulose I allomorphs is mere coincidence. This hemiacetal formation always means crosslinking, either intramolecular or intermolecular. At oxidation degrees below 100 %, the newly generated aldehyde groups can (in addition to C6) engage in hemiacetal formation with non-reacted C2 and C3 hydroxyls, thus temporarily impeding oxidation at those positions. At 100 % oxidation, only C6 is available for hemiacetal formation since all C2 and C3 (at least theoretically) have been consumed and converted to (masked) aldehydes.

This observation goes in hand with the observation that DAC of lower oxidation degrees is water-insoluble and shows very high molecular weights caused by crosslinking, while highly oxidized samples (oxidation degree above 80 %) become water-soluble again.

At those very high degrees of oxidation nearing 100 %, the crosslinking effect is overcompensated by chain cleavage and molecular weight decrease. However, if only (or mainly) C6 is available for hemiacetal crosslinking, intramolecular links will be strongly favored over intermolecular ones due to entropic reasons. With the C3 of the same "former" anhydroglucopyranose unit, five-membered (furanoid) rings are formed, with the C2 six-membered rings (1,4-dioxanes). Both are favored over alternative linear links or large-membered annular structures with neighboring chains, which also accounts for better solubility.

Two interesting features can be derived from the solid-state NMR spectra: The prominent resonances between 85 and 93 ppm are mainly due to aldehyde hydrates. The shift region agrees with those of low-molecular weight model compounds. C6-aldehyde-glucopyranose, mainly present as the aldehyde hydrate in aqueous medium, shows corresponding resonance at 88 ppm (Röhrling et al. 2002). Hemialdal structures between two aldehyde groups (i.e., "double" hemiacetals, which involve aldehyde hydrates in their formation, HO–CH(R)–O–CH(R′)–OH) are found around 97 ppm. These three peculiar solid-state NMR features of periodate-oxidized celluloses—(a) hemiacetals involving C6, (b) aldehyde hydrates and (c) hemialdals—are already present at low oxidation degrees. Although diagnostic of periodate-oxidized material, and thus representing an interesting and valuable analytical indicator, they render the common approaches for determining crystallinity with solid-state NMR obsolete.

In summary, solid-state NMR is largely—if not completely—unable to report crystallinities in periodate-oxidized samples since the spectral complexity present in non-oxidized samples is severely aggravated by the multitude of additional structures added by the oxidation process. Therefore, alternatives were required, and NIR, ATR-IR and Raman spectroscopy calibrated against WAXS were tested for their suitability for determining the CI of oxidized celluloses.

Near-infrared spectroscopy (NIR)

Estimation of crystallinity from NIR spectra was described by Basch et al. (1974), with the NIR ratio $H_{4760}/(H_{4760} + H_{5190})$ correlating with X-ray crystallinities. The band at 4760 cm^{-1} was attributed to O–H and C–H deformational modes and O–H stretching, and the one at 5190 cm^{-1} to hydrogen bonds between cellulosic hydroxyls and adsorbed water (cf. Fig. S4 in the supplement for the typical NIR spectra of an oxidation series). Thus, the moisture content affects the NIR-based ratio determination. Our samples were measured in one batch after careful conditioning and equilibration in the measuring room for 1 week. One advantage of this simple method is that the results are independent of the type of crystal lattice. However, the results are influenced by the crystallite size (Schwanninger et al. 2011). The NIR ratio calculated from the peak height showed a clear and continuous decrease in crystallinity upon progressive oxidation (cf. Table 1; Fig. 5 and Fig. S7 in the supplement). The NIR ratios were lower for the mercerized samples and viscose fibers than for the native cellulose sample.

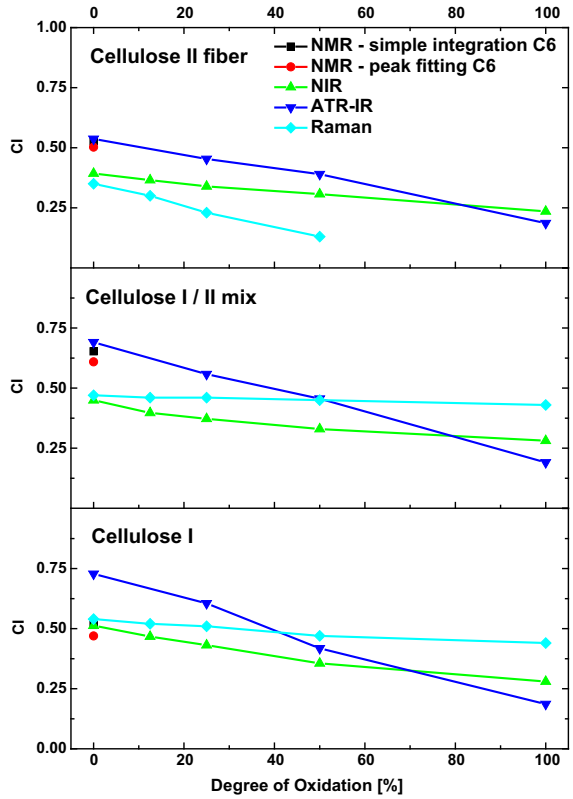

Fig. 5 Comparison of different crystallinity index determination methods for periodate oxidation series with: Cellulose I (pulp), Cellulose I/II mix (partly mercerized pulp) and Cellulose II fiber

Attenuated total reflection infrared spectroscopy (ATR-IR)

Mid-infrared spectra can also be used to determine crystallinity. Different bands have been proposed in the literature for that purpose. We used the ratio of the band at 1372 cm^{-1} to that at 2900 cm^{-1} since this method works well with cellulose I, cellulose II and mixtures of both. The band at 1372 cm^{-1} corresponds to the C–H bending mode, while that at 2900 cm^{-1} originates in C–H and CH_2 stretching vibrations (Nelson and O'Connor 1964).

In our study, the ATR-IR technique was used instead of the potassium bromide pellet technique since ATR-IR appeared to give more consistent results. The crystallinity indices were calculated from the peak heights and the peak areas. The peak height method showed a decrease in the CI with mercerization whereas the peak area method did not show significant changes. Both methods gave clearly lower CIs for the cellulose II fiber sample compared to the cellulose I sample. Periodate oxidation mainly caused a gradual decrease in the CI (cf. Table 1; Fig. 5 and Fig. S7 in the supplement). All fully oxidized samples showed the same CI, although the values did not decrease to zero. However, as seen in Fig. S5 (in the supplement), periodate oxidation affected the shape of the peaks used for calculating the CI. The reference band at 2900 cm^{-1} is deformed, and the peaks at 1370 and 1430 cm^{-1} merge to a certain extent. This makes the results more uncertain, in particular for higher degrees of oxidation.

Raman spectroscopy

Finally, Raman spectroscopy was also tested to determine the CI in the oxidized samples. According to the literature, the range from 1510 to 1210 cm^{-1} is highly dependent on crystallinity (Schenzel and Fischer 2004). Methylene bending vibrations cause characteristic bands for crystalline (1481 cm^{-1}) and amorphous (1462 cm^{-1}) cellulose. Two methods for calculating the CI have been published. One option is to calculate the peak height ratio of the crystalline ($I_{crystalline}$, I_c) and amorphous ($I_{amorphous}$, I_a) bands: $XcRaman\ [\%] = I_c/(I_c + I_a) * 100$. Another approach is to perform multivariate analysis that calibrates the Raman data with the WAXS results (Schenzel and Fischer 2004; Schenzel et al. 2005; Röder et al. 2006a, b).

The Raman spectra of the periodate oxidized samples deviated significantly from the spectrum of pure, unmodified cellulose, as expected (cf. Fig. S6 in the supplement). Therefore, the chemometric analyses results have a high level of uncertainty, especially in higher degrees of oxidation: The method gives 49 and 67 % cellulose I content for fully oxidized (nearly amorphous) cellulose II pulp samples.

Interestingly, in the range of lower oxidation degrees where the approach should retain a reasonable level of reliability, the cellulose I content increased for the cellulose I/II mixture samples. This agrees with the observation that cellulose II crystals are oxidized faster than their cellulose I counterparts. However, the reliability of the Raman approach for periodate-oxidized samples is not known, and conclusions must be drawn with caution.

Crystallinity indices calculated according to the chemometric method showed only a small decrease during oxidation for the cellulose I and mixed cellulose I/II samples. For cellulose II, a clear decrease in the CI was observed (cf. Table 1; Fig. 5 and Fig. S7 in the supplement).

In summary, the results depended on the method. Solid-state NMR was not suitable for oxidized samples due to severe changes in the spectra that made the CI calculations inaccurate, but nevertheless provided valuable results for structural motifs in oxidized cellulose. Crystallinity determinations with NIR and ATR-IR showed a clear decrease in crystallinity caused by periodate oxidation. However, some interference in the oxidation with the peaks used for calculating the CI were observed. These methods mainly showed lower crystallinity for the mercerized samples and viscose fibers compared to the cellulose I pulp samples. Thus, the faster reaction of cellulose II is not caused by faster oxidation of cellulose II crystals but by the higher amorphous content of the starting material and preferential oxidation of the amorphous phase. However, the Raman data showed the cellulose I portion increased during oxidation of the mixed cellulose I/II samples. Additionally, the CI calculated from the NMR of the non-oxidized samples did not show significantly lower crystallinity for the cellulose II fiber samples and even higher crystallinity for the mercerized samples compared to the cellulose I pulp. These findings indicate a faster attack of periodate on cellulose II crystals and contradicts the conclusion based on the IR techniques. Thus, we cannot give a

definite answer whether cellulose polymorphs behave differently in periodate oxidation. This is not due to kinetic inaccuracies, but to uncertainties and inter-method disagreements in determining the CI.

Thermogravimetric analysis

TGA was performed to check for possible differences in the thermostabilities of periodate-oxidized cellulose I and II. The first derivatives of the thermogravimetric curves were calculated to help interpret the data. In these derivative thermogravimetric analysis (DTGA) curves, the temperature ranges with the highest degradation rates are peaks. The samples used for TGA were air-dried. The mass loss up to 150 °C was caused by the varying moisture content of the samples. The most prominent degradation of non-oxidized samples occurred between 200 and 360 °C (see Fig. 6 top). The non-oxidized samples (see Fig. 7a and Table S1 in supplementary data) had two peaks above 150 °C in the DTGA curves. The first, most prominent peak (peak B) appeared around 330–340 °C. A second slower decomposition step was visible around 500 °C where peak C is located. This step was assigned to oxidative degradation of cellulose degradation products (Aggarwal et al. 1997). The TGA and DTGA curves of the partly and fully mercerized pulp samples were similar, but the mercerized samples had a slightly lower mass loss in the

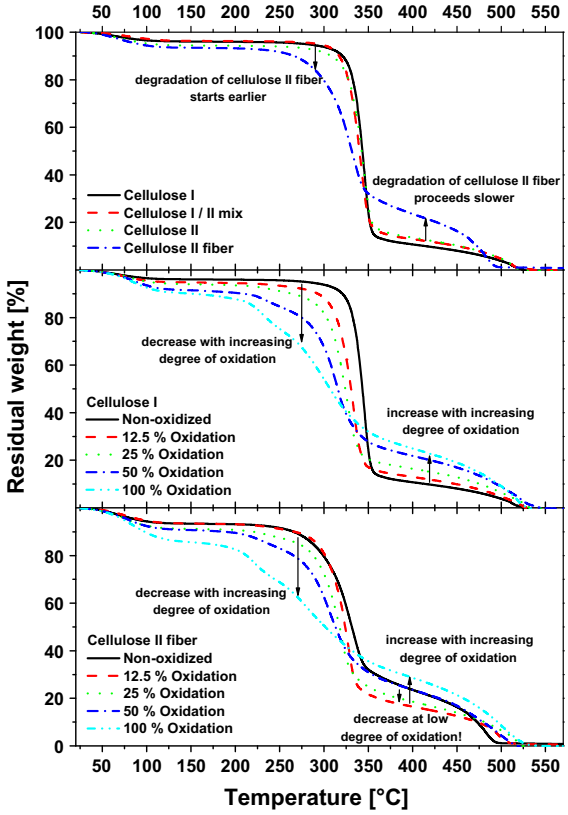

Fig. 6 Thermogravimetric analysis of: Non-oxidized samples; Oxidation series with cellulose I (pulp) and cellulose II fiber

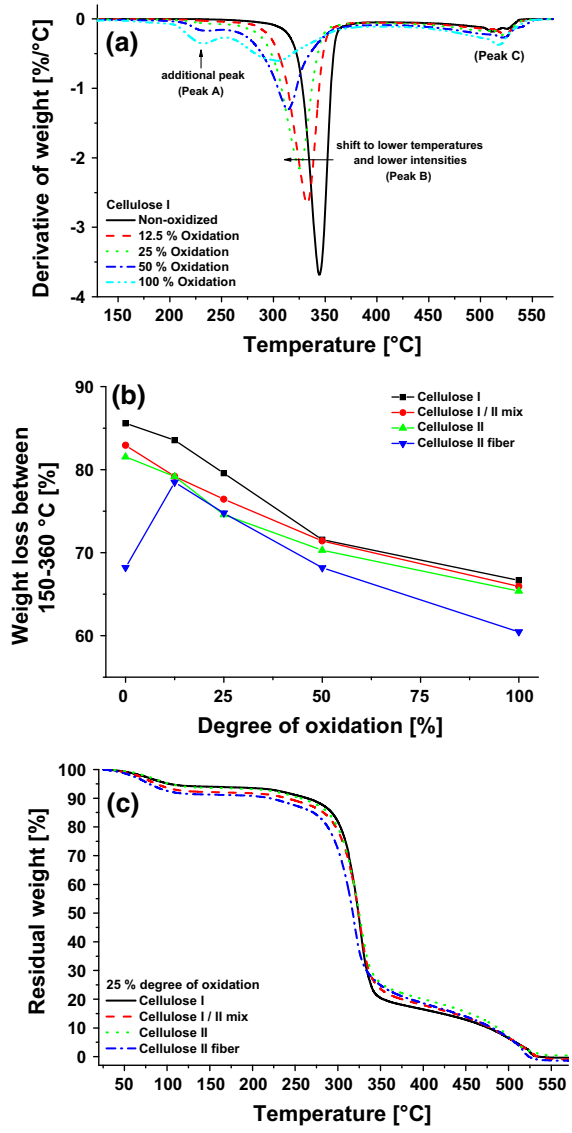

Fig. 7 **a** Derivative thermogravimetric analysis for cellulose I oxidation series; **b** weight loss in the temperature range from 150 to 360 °C; **c** Comparison of TGA curves of different cellulose samples with the same degree of oxidation (25 %)

temperature range 150–360 °C. This indicates that there are only small differences in the thermal decomposition of cellulose I and cellulose II polymorphs. However, the cellulose II fiber samples had a decomposition pattern different from that of the mercerized and non-mercerized cellulose I samples. The decomposition started earlier, but proceeded more slowly. This could be because the molar mass of the viscose fibers is much lower than that of the pulp samples or because the hemicelluloses located mainly in the outer layer of the viscose fibers started to decompose earlier than cellulose but formed charred protection layers that inhibit reaction and mass loss from more interior regions. Our findings differ somewhat from the literature that described mercerization of cotton decreased activation energy whereas viscose fibers had higher activation energy compared to mercerized cotton. The latter effect has been explained by the high orientation of the crystallites in viscose fibers (Sefain and El-Kalyoubi 1984). In periodate-oxidized material, thermostability decreased in the lower temperature range but increased in the higher temperature range (cf. Fig. 6 middle and bottom and Fig. S8a + b in the supplement). This causes an additional degradation peak (peak A around 220–230 °C), a shift of peak B toward lower temperatures (see Fig. 7a and Table S1 in the supplementary data), a lower weight loss at temperatures of 360 °C and above and a more pronounced peak C (cf. Fig. 7b). The shift toward lower degradation temperatures has been explained by the lower crystallinity of the oxidized samples and degradation reactions during periodate oxidation (Varma and Chavan 1995a; Vicini et al. 2004). Increased degradation around peak C has been attributed to oxidation of DAC to dicarboxylcellulose (Pataky et al. 1973).

Increased thermostability at high temperatures might be caused by the higher crosslinking ability of DAC compared to non-oxidized samples (Varma and Chavan 1995b). Our results for TGA with oxidized cellulose I are in good agreement with the literature. However, an unexpected behavior was found for cellulose II fibers (see Fig. 6 bottom, Fig. 7b). In the temperature range 350–450 °C, the slightly oxidized samples had lower residual weight compared to the non-oxidized samples. This effect is probably caused by the special structure (highly ordered, sheet-core structure etc.) of the viscose fibers that is then destroyed at the beginning of the oxidation, although higher degrees of oxidation decrease the weight loss due to crosslinking. The oxidized cellulose II fiber samples had similar TGA curves compared to the mercerized and non-mercerized pulp samples of the same degree of oxidation (see Fig. 7c).

Conclusion

Periodate oxidation proceeded significantly faster in the cellulose II samples (the pulp and viscose fibers) compared to the cellulose I samples. Crystallinity was measured to address the question whether this overall better accessibility of cellulose II is caused by lower crystallinity or by the higher reactivity of cellulose II crystals. However, this issue could not be finally clarified since different CI determination methods lead to different conclusions. The CPMAS NMR data indicate a faster oxidation of cellulose II due to an allomorph effect, whereas Raman (calibrated with WAXS) explained the higher reaction rates of the cellulose II samples just by their lower crystallinity. In any case, determining the CI of the periodate oxidized samples was problematic; in particular solid-state NMR failed due to significant superposition of resonances. Based on this study, we prefer the Raman approach as the best—although not fully satisfying—approach for CI determination for periodate-oxidized samples.

Thermogravimetric analysis did not show significant differences between non-oxidized cellulose polymorphs. In general, oxidation caused a decrease in the starting temperature of thermal degradation, but decomposition proceeded more slowly and the thermostability of the oxidized samples increased at temperatures higher than about 350 °C. Viscose fibers showed a different decomposition pattern: Degradation of the non-oxidized samples started at lower temperatures, but proceeded more slowly than in the case of the pulp samples. Interestingly, oxidation leveled out this effect, and the TGA curves of the oxidized viscose fibers were similar to the ones from the oxidized pulp samples.

Acknowledgments This work was funded by the Austrian Research Funding Association (FFG) under the scope of the COMET programs Process Analytical Chemistry (PAC) and Wood K plus with its industrial partner Kelheim Fibres GmbH. The FLIPPR research project and the companies and funding institution associated with it are gratefully acknowledged for

financial support. We thank Dr. T. Röder, Lenzing AG, for support with the Raman analysis.

References

Aggarwal P, Dollimore D, Heon K (1997) Comparative thermal analysis study of two biopolymers, starch and cellulose. J Therm Anal 50(1–2):7–17. doi:10.1007/bf01979545

Ahn K, Rosenau T, Potthast A (2013) The influence of alkaline reserve on the aging behavior of book papers. Cellulose 20(4):1989–2001. doi:10.1007/s10570-013-9978-3

Ant-Wuorinen O (1955) Evaluation of the crystallinity of cellulose from X-ray diffraction pictures. Pap Puu 37:335–368

Baldinger T, Moosbauer J, Sixta H (2000) Supermolecular structure of cellulosic materials by Fourier-transform infrared spectroscopy (FTIR) calibrated by WAXS and 13C NMR. Lenzing Ber 79:15–17

Basch A, Wasserman T, Lewin M (1974) Near-infrared spectrum of cellulose: a new method for obtaining crystallinity ratios. J Polym Sci A-1: Polym Chem 12(6):1143–1150. doi:10.1002/pol.1974.170120601

Calvini P, Conio G, Princi E, Vicini S, Pedemonte E (2006a) Viscometric determination of dialdehyde content in periodate oxycellulose Part II. Topochemistry of oxidation. Cellulose 13(5):571–579. doi:10.1007/s10570-005-9035-y

Calvini P, Gorassini A, Luciano G, Franceschi E (2006b) FTIR and WAXS analysis of periodate oxycellulose: evidence for a cluster mechanism of oxidation. Vib Spectrosc 40(2):177–183. doi:10.1016/j.vibspec.2005.08.004

Ciolacu D, Ciolacu F, Popa VI (2011) Amorphous cellulose: structure and characterization. Cell Chem Technol 45(1–2): 13–21

Coseri S, Biliuta G, Simionescu BC, Stana-Kleinschek K, Ribitsch V, Harabagiu V (2013) Oxidized cellulose—survey of the most recent achievements. Carbohydr Polym 93(1):207–215. doi:10.1016/j.carbpol.2012.03.086

Dash R, Elder T, Ragauskas A (2012) Grafting of model primary amine compounds to cellulose nanowhiskers through periodate oxidation. Cellulose 19(6):2069–2079. doi:10.1007/s10570-012-9769-2

Fan QG, Lewis DM, Tapley KN (2001) Characterization of cellulose aldehyde using Fourier transform infrared spectroscopy. J Appl Polym Sci 82(5):1195–1202. doi:10.1002/app.1953

Fink HP, Fanter D, Philipp B (1985) Röntgen-Weitwinkeluntersuchungen zur übermolekularen Struktur beim Cellulose-I–II-Phasenübergang. Acta Polym 36(1):1–8. doi:10.1002/actp.1985.010360101

Garvey CJ, Parker IH, Simon GP (2005) On the interpretation of X-ray diffraction powder patterns in terms of the nanostructure of cellulose I fibres. Macromol Chem Phys 206(15):1568–1575. doi:10.1002/macp.200500008

Henniges U, Kostic M, Borgards A, Rosenau T, Potthast A (2011) Dissolution behavior of different celluloses. Biomacromolecules 12(4):871–879. doi:10.1021/bm101555q

Henniges U, Okubayashi S, Rosenau T, Potthast A (2012) Irradiation of cellulosic pulps: understanding its impact on cellulose oxidation. Biomacromolecules 13(12):4171–4178. doi:10.1021/bm3014457

Hermans PH, Weidinger A (1948) Quantitative X-ray investigations on the crystallinity of cellulose fibers. A background analysis. J Appl Phys 19(5):491–506. doi:10.1063/1.1698162

Hudson BG, Barker R (1967) The overoxidation of carbohydrates with sodium metaperiodate. J Org Chem 32(7):2101–2109. doi:10.1021/jo01282a010

Isogai A, Kato Y (1998) Preparation of polyuronic acid from cellulose by TEMPO-mediated oxidation. Cellulose 5(3):153–164. doi:10.1023/a:1009208603673

Jackson EL, Hudson CS (1938) The structure of the products of the periodic acid oxidation of starch and cellulose. J Am Chem Soc 60(5):989–991. doi:10.1021/ja01272a001

Jayme G, Maris S (1944) Über die Oxydation der Cellulose mit gepufferter Perjodsäure und die Gewinnung von Abbauprodukten der oxydierten Cellulose. Berichte der deutschen chemischen Gesellschaft (A and B Series) 77(6–7):383–392. doi:10.1002/cber.19440770603

Kim U-J, Kuga S (2001) Thermal decomposition of dialdehyde cellulose and its nitrogen-containing derivatives. Thermochim Acta 369(1–2):79–85. doi:10.1016/S0040-6031(00)00734-6

Kim U-J, Kuga S, Wada M, Okano T (1999) Anomaly in periodate oxidation of crystalline cellulose. Am Chem Soc, pp CELL-041

Kim U-J, Kuga S, Wada M, Okano T, Kondo T (2000) Periodate oxidation of crystalline cellulose. Biomacromolecules 1(3):488–492. doi:10.1021/bm0000337

Larsson PT, Wickholm K, Iversen T (1997) A CP/MAS13C NMR investigation of molecular ordering in celluloses. Carbohydr Res 302(1–2):19–25. doi:10.1016/S0008-6215(97)00130-4

Larsson PT, Hult E-L, Wickholm K, Pettersson E, Iversen T (1999) CP/MAS 13C-NMR spectroscopy applied to structure and interaction studies on cellulose I. Solid State Nucl Magn Reson 15(1):31–40. doi:10.1016/S0926-2040(99)00044-2

Li H, Yang Y, Wen Y, Liu L (2007) A mechanism study on preparation of rayon based carbon fibers with $(NH_4)2SO_4$/NH_4Cl/organosilicon composite catalyst system. Compos Sci Technol 67(13):2675–2682. doi:10.1016/j.compscitech.2007.03.008

Liu X, Wang L, Song X, Song H, Zhao JR, Wang S (2012) A kinetic model for oxidative degradation of bagasse pulp fiber by sodium periodate. Carbohydr Polym 90(1):218–223. doi:10.1016/j.carbpol.2012.05.027

Maekawa E, Kosaki T, Koshijima T (1986) Periodate oxidation of mercerized cellulose and regenerated cellulose. Wood Res: Bull Wood Res Inst Kyoto Univ 73:44–49

Malaprade L (1928) Action of polyalcohols on periodic acid. Analytical application. Bull Soc Chim Fr 43:683–696

Margutti S, Vicini S, Proietti N, Capitani D, Conio G, Pedemonte E, Segre AL (2002) Physical–chemical characterisation of acrylic polymers grafted on cellulose. Polymer 43(23):6183–6194. doi:10.1016/S0032-3861(02)00533-5

Massiot D, Fayon F, Capron M, King I, Le Calvé S, Alonso B, Durand J-O, Bujoli B, Gan Z, Hoatson G (2002) Modelling one- and two-dimensional solid-state NMR spectra. Magn Reson Chem 40(1):70–76. doi:10.1002/mrc.984

Meng S, Feng Y, Liang Z, Fu Q, Zhang E (2005) Oxidizing cellulose to 2,3-dialdehyde cellulose by sodium periodate. Trans Tianjin Univ 11:250–254

Nelson ML, O'Connor RT (1964) Relation of certain infrared bands to cellulose crystallinity and crystal lattice type. Part II. A new infrared ratio for estimation of crystallinity in celluloses I and II. J Appl Polym Sci 8(3):1325–1341. doi:10.1002/app.1964.070080323

Newman RH (2004) Homogeneity in cellulose crystallinity between samples of Pinus radiata wood. Holzforschung 58(1):91–96. doi:10.1515/HF.2004.012

Park S, Johnson D, Ishizawa C, Parilla P, Davis M (2009) Measuring the crystallinity index of cellulose by solid state 13C nuclear magnetic resonance. Cellulose 16(4):641–647. doi:10.1007/s10570-009-9321-1

Park S, Baker JO, Himmel ME, Parilla PA, Johnson DK (2010) Cellulose crystallinity index: measurement techniques and their impact on interpreting cellulase performance. Biotechnol Biofuels. doi:10.1186/1754-6834-3-10

Pataky B, Perczel S, Sachetto JP (1973) The structural characterization of oxidized celluloses by thermogravimetric analysis. J Polym Sci Polym Symp 43(1):267–275. doi:10.1002/polc.5070430123

Potthast A, Röhrling J, Rosenau T, Borgards A, Sixta H, Kosma P (2003) A novel method for the determination of carbonyl groups in cellulosics by fluorescence labeling. 3. Monitoring oxidative processes. Biomacromolecules 4(3):743–749. doi:10.1021/bm025759c

Potthast A, Kostic M, Schiehser S, Kosma P, Rosenau T (2007) Studies on oxidative modifications of cellulose in the periodate system: molecular weight distribution and carbonyl group profiles. Holzforschung 61(6):662–667. doi:10.1515/hf.2007.099

Proietti N, Capitani D, Pedemonte E, Blümich B, Segre AL (2004) Monitoring degradation in paper: non-invasive analysis by unilateral NMR. Part II. J Magn Reson 170(1):113–120. doi:10.1016/j.jmr.2004.06.006

Ranby BG (1952) The mercerisation of cellulose. I. A thermodynamic discussion. Acta Chem Scand 6:101–115. doi:10.3891/acta.chem.scand.06-0101

Röder T, Moosbauer J, Fasching M, Bohn A, Fink H-P, Baldinger T, Sixta H (2006a) Crystallinity determination of man-made cellulose fibers—comparison of analytical methods. Lenzing Ber 86:132–136

Röder T, Moosbauer J, Fasching M, Bohn A, Fink H-P, Baldinger T, Sixta H (2006b) Crystallinity determination of native cellulose—comparison of analytical methods. Lenzing Ber 86:85–89

Röhrling J, Potthast A, Lange T, Rosenau T, Adorjan I, Hofinger A, Kosma P (2002) Synthesis of oxidized methyl 4-*O*-methyl-β-D-glucopyranoside and methyl β-D-glucopyranosyl-(1 → 4)-β-D-glucopyranoside derivatives as substrates for fluorescence labeling reactions. Carbohydr Res 337(8):691–700. doi:10.1016/S0008-6215(02)00048-4

Rowland SP, Cousins ER (1966) Periodate oxidative decrystallization of cotton cellulose. J Polym Sci A-1: Polym Chem 4(4):793–799. doi:10.1002/pol.1966.150040406

Saito T, Isogai A (2004) TEMPO-mediated oxidation of native cellulose. The effect of oxidation conditions on chemical and crystal structures of the water-insoluble fractions. Biomacromolecules 5(5):1983–1989. doi:10.1021/bm0497769

Schenzel K, Fischer S (2004) Applications of FT Raman spectroscopy for characterization of cellulose. Lenzing Ber 83:67–70

Schenzel K, Fischer S, Brendler E (2005) New method for determining the degree of cellulose I crystallinity by means of FT Raman spectroscopy. Cellulose 12(3):223–231. doi:10.1007/s10570-004-3885-6

Schwanninger M, Rodrigues J, Fackler K (2011) A review of band assignments in near infrared spectra of wood and wood components. J Near Infrared Spectrosc 19(5):287–308. doi:10.1255/jnirs.955

Sefain MZ, El-Kalyoubi SF (1984) Thermogravimetric studies of different celluloses. Thermochim Acta 75(1–2):107–113. doi:10.1016/0040-6031(84)85010-8

Segal L, Creely JJ, Martin AE, Conrad CM (1959) An empirical method for estimating the degree of crystallinity of native cellulose using the X-ray diffractometer. Text Res J 29(10):786–794. doi:10.1177/004051755902901003

Shafizadeh F (1982) Introduction to pyrolysis of biomass. J Anal Appl Pyrol 3(4):283–305. doi:10.1016/0165-2370(82)80017-X

Siller M, Ahn K, Pircher N, Rosenau T, Potthast A (2014) Dissolution of rayon fibers for size exclusion chromatography: a challenge. Cellulose 21(5):3291–3301. doi:10.1007/s10570-014-0356-6

Sirvio J, Hyvakko U, Liimatainen H, Niinimaki J, Hormi O (2011) Periodate oxidation of cellulose at elevated temperatures using metal salts as cellulose activators. Carbohydr Polym 83(3):1293–1297. doi:10.1016/j.carbpol.2010.09.036

Stefanovic B, Rosenau T, Potthast A (2013) Effect of sonochemical treatments on the integrity and oxidation state of cellulose. Carbohydr Polym 92(1):921–927. doi:10.1016/j.carbpol.2012.09.039

Symons MCR (1955) Evidence for formation of free-radical intermediates in some reactions involving periodate. J Chem Soc (Resumed). doi:10.1039/JR9550002794

Tang MM, Bacon R (1964) Carbonization of cellulose fibers—I. Low temperature pyrolysis. Carbon 2(3):211–220. doi:10.1016/0008-6223(64)90035-1

Varma AJ, Chavan VB (1995a) A study of crystallinity changes in oxidised celluloses. Polym Degrad Stab 49(2):245–250. doi:10.1016/0141-3910(95)87006-7

Varma AJ, Chavan VB (1995b) Thermal properties of oxidized cellulose. Cellulose 2(1):41–49. doi:10.1007/BF00812771

Varma AJ, Kulkarni MP (2002) Oxidation of cellulose under controlled conditions. Polym Degrad Stab 77(1):25–27. doi:10.1016/S0141-3910(02)00073-3

Varma AJ, Jamdade YK, Nadkarni VM (1985) Wide-angle X-ray diffraction study of the effect of periodate oxidation and thermal treatment on the structure of cellulose powder. Polym Degrad Stab 13(1):91–98. doi:10.1016/0141-3910(85)90135-1

Varma AJ, Chavan VB, Rajmohanan PR, Ganapathy S (1997) Some observations on the high-resolution solid-state CP-MAS 13C-NMR spectra of periodate-oxidised cellulose. Polym Degrad Stab 58(3):257–260. doi:10.1016/S0141-3910(97)00049-9

Vicini S, Princi E, Luciano G, Franceschi E, Pedemonte E, Oldak D, Kaczmarek H, Sionkowska A (2004) Thermal analysis and characterisation of cellulose oxidised with sodium

methaperiodate. Thermochim Acta 418(1–2):123–130. doi:10.1016/j.tca.2003.11.049

Vonk C (1973) Computerization of Ruland's X-ray method for determination of the crystallinity in polymers. J Appl Crystallogr 6(2):148–152. doi:10.1107/S0021889873008332

Whistler RL, Chang PK, Richards GN (1959) Alkaline degradation of periodate-oxidized starch. J Am Chem Soc 81(12):3133–3136. doi:10.1021/ja01521a054

Wickholm K, Larsson PT, Iversen T (1998) Assignment of non-crystalline forms in cellulose I by CP/MAS 13C NMR spectroscopy. Carbohydr Res 312(3):123–129. doi:10.1016/S0008-6215(98)00236-5

Xu YH, Huang C (2011) Effect of sodium periodate selective oxidation on crystallinity of cotton cellulose. Adv Mater Res. doi:10.4028/www.scientific.net/AMR.197-198.1201

Zuckerstätter G, Schild G, Wollboldt P, Roeder T, Weber HK, Sixta H (2009) The elucidation of cellulose supramolecular structure by 13C CP-MAS NMR. Lenzing Ber 87:38–46